Spoof Surface Plasmon Antenna for IoT Application

Mohamed M. Gad, *Student Member, IEEE*, Mai O. Sallam, Senior Member, *IEEE*

***Abstract*—This report presents the main results of the project, which focuses on developing a miniaturized antenna using Spoof Surface Plasmon Polaritons (SSPPs) loading. To study miniaturization of complex antenna arrays, the design of an SSPPs traveling wave antenna is presented. The dispersion diagram of the SSPPs-loaded microstrip is presented using the eigen mode solver in CST Microwave Studio, illustrating the reduction in the phase constant of the microstrip line. To evaluate the impact of the loading, both the original and the SSPPs-loaded microstrip lines are analyzed in the context of a single dipole antenna. Subsequently, the final proposed antenna design incorporating the SSPPs structure is presented.**

***Index Terms*—Spoof Surface Plasmon Polaritons (SSPPs), dispersion diagram, Traveling Wave Antennas (TWAs), Antenna miniaturization**

I. INTRODUCTION

Surface Plasmon Polariton (SPP) is a phenomenon where light interaction occurs at the metal/dielectric interface. This interaction causes a collective oscillation of electrons known as surface polaritons which occur at very high frequencies (optical range). This natural phenomenon leads to the miniaturization of plasmonic devices such as nano antennas and plasmonic sensors. For radio, microwave and millimeter wave frequencies, SPPs are not supported since metals are highly conductive. Nevertheless, “SPPs-like” waves, which are referred to as Spoof Surface Plasmons Polaritons (SSPPs), can be excited using subwavelength periodic corrugated structures to achieve the same goal of antenna miniaturization. This idea was first proposed by Pendry et al. in [1].

Despite the large number of studies employing this concept in the THz regime, limited research has considered the design of SSPPs for antenna miniaturization at lower frequency ranges. Various miniaturization methods and approaches have been suggested, including antennas based on space-filling curves such as fractal antennas [2]. However, they do not overcome the fundamental limits on bandwidth and efficiency. Other techniques, such as reactively loaded antennas using periodic lumped capacitance [3] and slow-wave antennas based on periodic loading of SSPPs stubs [4], are effective through modifying the guided wavelength of the transmission line.

The authors in [5] developed a miniaturized version of a dipole antenna at 2.4 GHz using stubs to excite SSPPs. The antenna size was reduced to almost 80% of its traditional dimensions as the result of the reduced guided wavelength. In [6] a novel low profile SSPPs monopole antenna is designed to reduce the monopole arm length from 28.5 to 14.7 mm resulting in substantial area saving. Despite the growing interest in SSPP structures, limited research has been conducted on the miniaturization of antenna arrays using SSPP-based transmission lines.

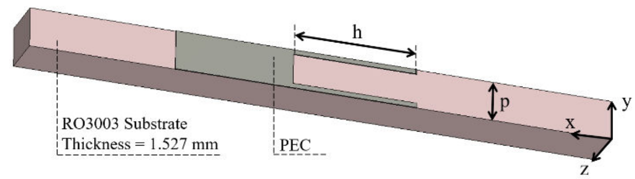

Fig. 1. SSPPS-loaded microstrip line unit cell.

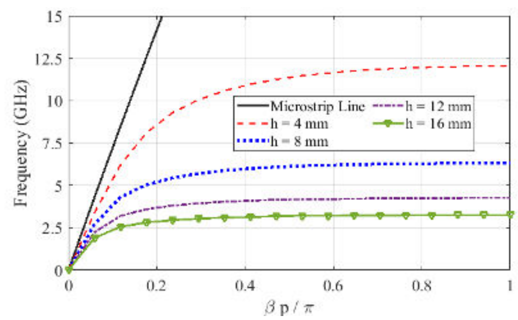

Fig. 2. Dispersion diagram of SSPPs-loaded microstrip lines.

II. DISPERSION ENGINEERING

The typical configuration of the SSPP unit cell that forms the radiator is shown in Fig. 1. The structure consists of a segment of a microstrip line loaded with periodic metallic strips of width 0.3 mm and length h. Since only a single unit cell is simulated, it includes two metallic strips, each having width 0.15 mm (i.e., half the full strip width), placed at the ends to satisfy periodicity with a period p = 1.3 mm. The structure is periodic along the y-direction; hence, periodic boundary conditions are applied to both $-y$ and $+y$ faces. To confine the mode within the simulation domain, Perfect Electric Conductor (PEC) boundary conditions (i.e., $E_t = 0$) are assigned to the $-x$, $+x$, $-z$, and $+z$ planes. The simulation domain includes an air region that extends above the SSPP microstrip structure along the $-z$-direction to better capture field interactions above the line.

To illustrate the dispersion behavior of the proposed structure, the resulting dispersion diagram is shown in Fig. 2. The figure demonstrates how changes in the strip height, h, affect the dispersion behavior of the SSPPs transmission line. As h increases the transmission phase is reduced at a given frequency, implying that a shorter structure length is needed to achieve the same phase shift. This slow-wave behavior allows the guided wavelength to be significantly reduced compared to a conventional microstrip line operating at the same frequency.

To illustrate the impact of SSPP loading, a single-element dipole antenna is simulated under three different configurations. In the first case, a conventional dipole antenna with a length of 50 mm, corresponding to approximately half the guided wavelength, is analyzed as a reference. In the second

Mohamed M. Gad is with the Nanoelectronics Integrated Systems Center (NISC), Nile University, Giza 12588, Egypt (m.magdy2212@ nu.edu.eg).

Mai O. Sallam is with the Nanoelectronics Integrated Systems Center (NISC), Nile University, Giza 12588, Egypt (masallam@nu.edu.eg).

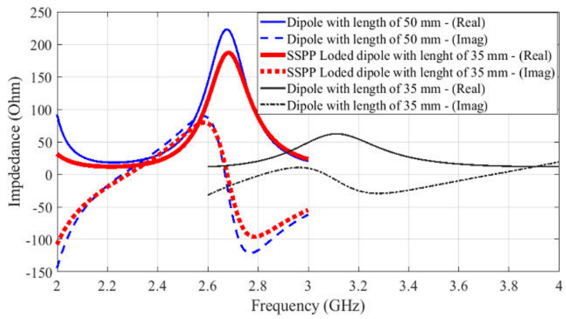

Fig. 3. Input impedance of dipoles with/without loading

case, the same dipole is modified by incorporating SSPPs stubs, reducing the total length to 35 mm. Finally, a third configuration simulates the same 35 mm dipole without SSPP loading to evaluate the effect of size reduction solely. The height *h*, is set to 9.1 mm. Fig. 3 presents the simulated input impedance for the three antenna configurations, including both real and imaginary components. Notably, the SSPP-loaded dipole with a length of 35 mm exhibits a resonance frequency and impedance profile closely matching those of the 50 mm unloaded dipole, in both the real and imaginary components, without compromising the resonance characteristics.

II. Proposed SSPPs-Loaded TWA Design

Fig. 4 shows the proposed SSPPs-loaded design. The description and dimensional parameters for the unloaded TWA design can be found in our previous work [7]. Each dipole is loaded with a periodic array of metallic strips forming the SSPP structure, and the dipoles are interconnected using connectors similar to those in the unloaded version. Each unit cell of the SSPP comprises a set of thin copper strips of width, w_i, spacing, s_i, and length, h_i, where the subscript "i" denotes the order of the radiator along the antenna structure. The entire structure is implemented on a Rogers 3003 substrate for fair comparison with the unloaded design. The SSPPs antenna achieves a more compact structure. The overall lateral dimensions are reduced to 46 mm × 95 mm × 1.527 mm, with a shortened effective radiator length of 35 mm compared to the original 50 mm design. The reduction factor is 20.54% with respect to the original structure. The gap s_i between the strips in the first dipole element is 1.258 mm, while in the remaining elements, it is set to 1 mm. The width of each strip is uniformly fixed at s_w = 0.3 mm. The lengths of the SSPP loading strips, h_i, are 9.1 mm, 5.8 mm, 5.7 mm, 5.6 mm, 5.5 mm, 5.4 mm, and 5.3 mm, respectively.

II. Results and Discussions

For the SSPPs-loaded meander line antenna, the reflection coefficient and end-fire gain obtained using CST and HFSS are illustrated in Fig. 5 (a) and (b), respectively. The results show a matched bandwidth ranging from 2.21 to 2.69 GHz (2.21–2.71 GHz) based on CST (HFSS) simulations. This corresponds to a fractional bandwidth of 19.5% and 20.3%, as predicted by CST and HFSS, respectively. This implies that similar performance can be achieved for the unloaded structure as well. The CST and HFSS gain values show excellent agreement across the entire bandwidth. For consistency, the proposed model is compared with the original reference design based on HFSS

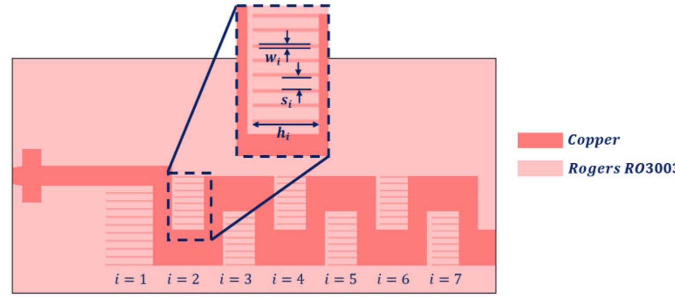

Fig. 4. Geometry of the proposed SSPPs-loaded TWA.

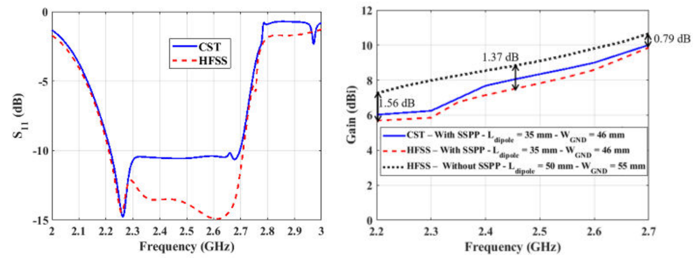

(a) (b)

Fig. 5. Results of the proposed SSPPs-loaded antenna. (a) reflection coefficient, and (b) end-fire gain.

simulations, as the HFSS results closely match the measured data of the original antenna. The results reveal a gain reduction of only 0.79 dB at the highest frequency of 2.7 GHz. At 2.2 GHz, the degradation is more pronounced, reaching 1.56 dB. This level of degradation is acceptable when considering the significant miniaturization achieved by reducing the dipole length, *L,* from 50 mm to 35 mm.

V. Conclusion

In conclusion**,** this project has allowed me to explore the field of spoof surface plasmon antennas, building on my previous work in dispersion engineering within photonics. The resulting design—a highly compact, high-gain antenna—constitutes a central part of my Master's thesis, which was completed in May 2025. This research has inspired me to pursue a PhD in computational electromagnetics, focusing on the development of an in-house solver for microstrip line analysis using the Method of Moments. I will begin my PhD studies at McMaster University in January 2026.

References

[1] Pendry JB, Martin-Moreno L, Garcia-Vidal FJ. Mimicking surface plasmons with structured surfaces. science. 2004 Aug 6;305(5685):847-8.

[2] Mohammed JR. A novel linear and planar multiband fractal-shaped antenna arrays with low sidelobes. International Journal of Communication Systems. 2024 Feb 11:e5736.

[3] Shen, Xiumei, et al. "Decoupling of two strongly coupled dual-band antennas with reactively loaded dummy element array." IEEE Access 7 (2019): 154672-154682.

[4] Mohammed JR. A novel linear and planar multiband fractal-shaped antenna arrays with low sidelobes. International Journal of Communication Systems. 2024 Feb 11:e5736.

[5] Y. Yang, Z. Li, S. Wang, X. Chen, J. Wang, and Y. J. Guo, "Miniaturized high order-mode dipole antennas based on spoof surface plasmon polaritons," IEEE Antennas and Wireless Propagation Letters, vol. 17, no. 12, pp. 2409–2413, 2018.

[6] Qu, Bingyue, et al. "Miniaturization of monopole antenna based on spoof surface plasmon polaritons." IEEE Antennas and Wireless Propagation Letters 20.8 (2021): 1562-1566.

[7] Gad, M.M., Sallam, M.O. High gain antipodal meander line antenna for point-to-point WLAN/WiMAX applications. Sci Rep 14, 5769 (2024). https://doi.org/10.1038/s41598-024-54994-x